Chemical Science

ROYAL SOCIETY OF CHEMISTRY

EDGE ARTICLE

View Article Online
View Journal

Cite this: DOI: 10.1039/d5sc09340f

All publication charges for this article have been paid for by the Royal Society of Chemistry

Zincafluorene complex with an empty C–Zn π orbital that captures visible light

Hidemitsu Iwamoto,[a] Yusuke Sunada [ab] and Yoshimasa Wada *[ab]

Zinc complexes are attractive candidates for photofunctional materials owing to the low cost and benign nature of Zn, yet directly engaging Zn orbitals in visible-light responses has remained elusive in mononuclear systems. Here, we realize this by engineering an empty C–Zn π orbital as the LUMO in carbene–zincafluorene frameworks, as demonstrated in three newly designed mononuclear Zn complexes. Selective recrystallization of one complex afforded two conformational polymorphs, enabling us to establish a clear correlation among carbene–zincafluorene coplanarity, formation of the empty C–Zn π orbital, LUMO lowering, and visible-light absorption. Natural atomic orbital analyses of the complexes indicate that tuning the carbene scaffold improves C(2p)/Zn(4p) energy-level matching and thereby increases Zn(4p) participation in the LUMO. Additionally, one complex exhibits bright room-temperature phosphorescence in the solid state with a PL quantum yield of 21% and an emission lifetime of 2.0 ms; theoretical calculations including spin–orbit coupling identify the Zn center as a key contributor to the emission. As a proof-of-concept for visible-light responsive photofunctional application, the same complex catalyzes stilbene isomerization under blue-LED irradiation. These results highlight the non-innocent role of Zn in visible-light responses and pave the way toward photoactive mononuclear Zn complexes.

Received 29th November 2025
Accepted 14th January 2026

DOI: 10.1039/d5sc09340f

rsc.li/chemical-science

Introduction

Metal complexes with d-block elements at their core have a wide range of functionalities,[1–4] particularly in photophysical and photochemical applications, because of the unique electronic transitions of their d electrons. In particular, d^{10} metal complexes have stable electronically excited states with metal-to-ligand charge transfer (MLCT) character, which has sparked interest in their application as photofunctional materials, especially for visible-light applications. Because of the increasing demand for sustainable and economically viable photofunctional materials, there has been growing interest in using 3d metals as affordable and earth-abundant alternatives to their 4d and 5d counterparts.[5,6] Although 3d metal complexes based on Cu, a group 11 element, have been studied extensively for visible-light photofunctional materials,[7–15] those based on inexpensive, low-toxicity Zn (a group 12 element) remain comparatively limited, even though both Cu(I) and Zn(II) possess a d^{10} electron configuration. Zn(II) complexes are typically colorless owing to a wide energy gap between the filled Zn 3d and empty 4s/4p orbitals, which renders electronic transitions involving Zn orbitals challenging in relatively low-energy visible light.[16,17] Consequently, the visible-light absorption of Zn(II)-based compounds has mostly depended on ligands, *i.e.*, ligand-centered (LC), intraligand charge transfer (ILCT) or ligand-to-ligand charge-transfer (LLCT) transitions,[18–26] and the role of the Zn center has generally been structural.

Recently, we have explored Zn complexes, focusing on the direct involvement of Zn orbitals in visible-light absorption and the resulting photofunctional behavior. By engineering two low-coordinate Zn(II) atoms in close proximity, we discovered that the interaction of the empty p orbitals of the Zn(II) centers forms stable σ-type orbitals, which serve as the lowest unoccupied molecular orbital (LUMO) responsible for visible-light absorption.[27] In this dinuclear complex, the Zn-centered orbitals were found to accelerate spin–flip electronic transitions; a Cd dinuclear analogue further underscored the decisive role of the metal center in facilitating such spin–flip processes.[28] Thus, when metal-centered orbitals directly participate in the excited states, the metal center can actively modulate the photophysical properties and endow the complex with unique photofunctionality. Based on these advancements, we next set out to tackle the challenge of designing mononuclear Zn complexes in which Zn orbitals non-innocently contribute to visible-light absorption. However, this is not a straightforward extension of the dinuclear cases but a substantive leap, as the key metal–metal orbital interaction that enables visible-light absorption in the dinuclear systems is fundamentally absent in mononuclear complexes. While two proximal Zn(II) centers enable interaction

[a]*Department of Applied Chemistry, School of Engineering, The University of Tokyo, 4-6-1 Komaba, Meguro-ku, Tokyo 153-8505, Japan. E-mail: waday@iis.u-tokyo.ac.jp*
[b]*Institute of Industrial Science, The University of Tokyo, 4-6-1 Komaba, Meguro-ku, Tokyo 153-8505, Japan*

between isoenergetic empty p orbitals to produce a low-energy σ-type LUMO, a single Zn center lacks such metal–metal interaction. Therefore, realizing visible-light absorption with explicit Zn-orbital participation in mononuclear systems requires engineering a distinctive LUMO that incorporates the intrinsically high-energy empty orbitals of Zn through tailored molecular design.

Meanwhile, Marian, Steffen, and co-workers have advanced the photophysics of Zn(II) complexes by re-examining previously reported emitters and dissecting their behavior with detailed theoretical calculations,[29,30] and by proposing computation-guided molecular-design strategies for emitters.[31] In particular, they established a fundamentally different class of Zn emitters using electron-accepting carbenes,[32,33] in which the lowest excited states exhibit LLCT with an unusual LMCT admixture, such that the Zn 4s/4p character[31] may contribute to the excited states. Although these carbene complexes were first realized as dimeric Zn systems, they more recently reported mononuclear Zn complexes stabilized in a trigonal structure by bulkier carbenes,[34,35] and some of these monomers display outstanding TADF performance.[35] However, for the mononuclear systems studied so far, the lowest-energy excitations are typically attributed to ligand-based transitions,[34,35] and a low-energy visible-light absorption that evidently involves the Zn center has not been demonstrated. Their prior theoretical work indicates that Zn-orbital mixing into low-lying excited states is possible under specific electronic conditions,[31] yet, to our knowledge, an experimentally verified mononuclear Zn complex showing clear Zn-orbital involvement in the visible-light absorption remains elusive. Addressing this gap is essential to deepen our understanding of the Zn center's role in photophysical behavior and to advance the visible-light photofunctions of Zn complexes; the need for such systems motivated the present study.

Here, we report mononuclear Zn systems that realize visible-light absorption involving Zn orbitals. We designed and synthesized three Zn complexes, **Z-cAAC^{Cy}**, **Z-SIP** and **Z-IP**, based on a zincafluorene scaffold with cyclic carbenes, anticipating the formation of low-energy empty C–Zn π orbitals that enable visible-light absorption through explicit Zn-orbital participation (*vide infra*). These complexes were characterized by using single-crystal X-ray diffraction (SC-XRD), NMR spectroscopy, photophysical measurements, and theoretical calculations. In particular, selective recrystallization of **Z-cAAC^{Cy}** afforded two conformational polymorphs, allowing us to correlate experimentally the formation of the C–Zn π orbital with the lowering of excited-state energy, facilitating visible-light absorption. In addition, because the complexes are composed only of H, C, and N atoms, with Zn as the only heavy atom, we successfully isolated the heavy-atom effects of the Zn center, elucidating its effects on the photoluminescence properties. Finally, taking advantage of the long-lived bright triplet state of **Z-IP**, we evaluated a representative triplet energy-transfer photocatalytic isomerization of stilbenes under blue LED irradiation, thereby confirming the non-innocent role of the Zn center in visible-light-driven photofunctionality.

Results and discussion

The synthetic procedures and characterization of **Z-cAAC^{Cy}**, **Z-SIP** and **Z-IP** (Fig. 1a) are detailed in the SI. In this study, we employed one cyclic(alkyl)(amino)carbene (cAAC) and two N-heterocyclic carbenes (NHCs) as carbene ligands. The complexes were fully characterized by SC-XRD, elemental analysis, and ^{1}H and ^{13}C NMR spectroscopy. Here, we first focused on the **Z-cAAC^{Cy}** complex. During recrystallization, two types of crystals were obtained depending on the solvent: colorless and yellow crystals. SC-XRD revealed that the colorless crystal adopts a perpendicular molecular geometry (**Z-cAAC$^{Cy}{}_{\perp}$**), in which the five-membered ring of the carbene ligand (shown in blue in Fig. 1b) is oriented nearly orthogonal to that of the zincafluorene ring (shown in red in Fig. 1b), with a dihedral angle (ω) between their best planes of 83.1°, whereas the yellow crystal exhibits a rather coplanar geometry with a ω value of 23.9° (**Z-cAAC$^{Cy}{}_{\parallel}$**) (Fig. 1b). The diffuse reflectance spectroscopy revealed that **Z-cAAC$^{Cy}{}_{\perp}$** displays an absorption onset around 430 nm, while **Z-cAAC$^{Cy}{}_{\parallel}$** exhibits an absorption band extending to approximately 500 nm in the visible-light region. Theoretical calculations[36] revealed that the ground state (S_0) → lowest singlet excited state (S_1) transition for **Z-cAAC$^{Cy}{}_{\perp}$** occurs at 399 nm, whereas that for **Z-cAAC$^{Cy}{}_{\parallel}$** appears at 506 nm (Tables S8 and S9). Examination of the molecular orbitals associated with these transitions revealed a marked difference in the LUMO character: **Z-cAAC$^{Cy}{}_{\parallel}$** uniquely forms an empty π-type orbital delocalized over the C–Zn bond, whose energy level is notably lowered by 0.32 eV compared with that of **Z-cAAC$^{Cy}{}_{\perp}$**

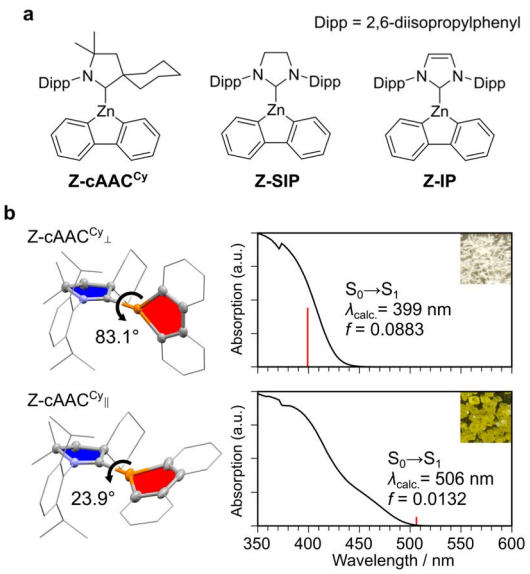

Fig. 1 (a) Chemical structure of **Z-cAAC^{Cy}**, **Z-SIP** and **Z-IP**. (b) Molecular structures of **Z-cAAC$^{Cy}{}_{\perp}$** and **Z-cAAC$^{Cy}{}_{\parallel}$** determined by SC-XRD (left) and their diffuse reflectance spectra together with photographs of the crystals under ambient light (right). Dihedral angle (ω) between the two best-planes defined by five-membered rings (as depicted by thermal ellipsoids at 50% probability) is also shown on the left. The calculated $S_0 \rightarrow S_1$ transition is indicated by red bars on the right together with their properties.

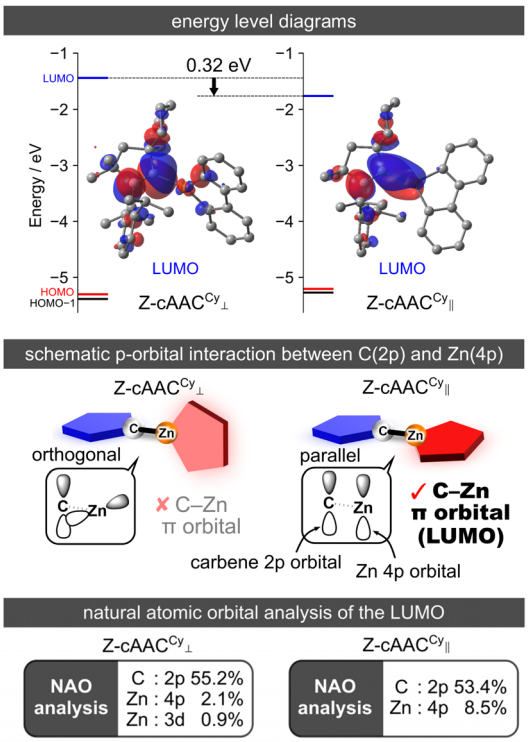

Fig. 2 Energy level diagrams and the LUMO distributions (top), schematic representation of p-orbital interaction responsible for forming the LUMO between C(2p) and Zn(4p) (middle), and natural atomic orbital (NAO) analysis of the LUMO (bottom) for **Z-cAAC$^{Cy}_{\perp}$** and **Z-cAAC$^{Cy}_{\parallel}$**. The isosurface value of the LUMO is 0.03. In the middle figure, the schematic representation of the five-membered ring of the carbene ligand and zincafluorene ring is shown in blue and red, respectively.

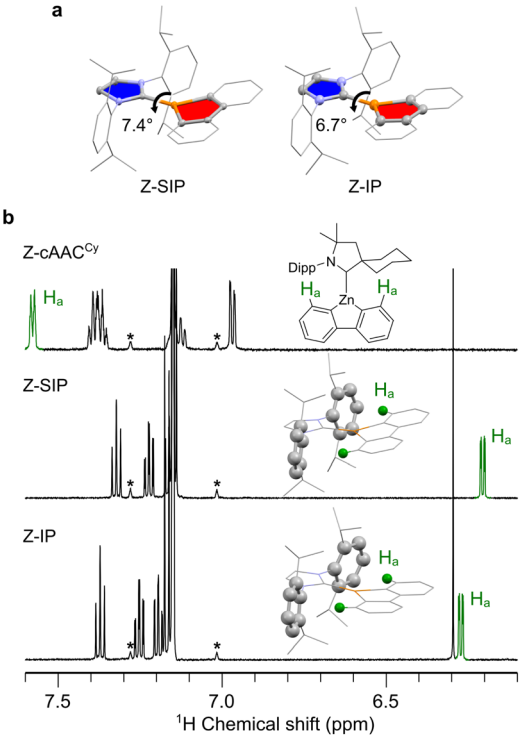

Fig. 3 (a) Selected molecular structures and ω values of **Z-SIP** (left) and **Z-IP** (right) determined by SC-XRD with five-membered rings depicted by thermal ellipsoids at 50% probability. (b) Aromatic regions of the ^{1}H NMR spectra of **Z-cAAC^{Cy}** (top), **Z-SIP** (middle) and **Z-IP** (bottom) in C_6D_6 and their molecular structures. Asterisk (*) denotes ^{13}C satellite peaks of the residual deuterated solvent. The phenyl rings of Dipp and specific hydrogen atoms (H_a) are shown in the ball-and-stick style. Green balls represent the H_a atoms.

(Fig. 2). Natural atomic orbital (NAO) analysis revealed a clear difference in the LUMO composition between the two conformational polymorphs. In **Z-cAAC$^{Cy}_{\perp}$**, the LUMO is mainly localized on the 2p orbital of the carbene carbon, with only 2.1% contribution from Zn 4p.[37] In contrast, **Z-cAAC$^{Cy}_{\parallel}$** features a distinct C–Zn π orbital with a markedly increased Zn 4p character (8.5%). Thus, both experimental and theoretical results demonstrate that coplanarity is critical for the formation of the empty C–Zn π orbital, which in turn facilitates low-energy visible-light absorption. Upon dissolution, however, both colorless and yellow crystals afforded the same yellow solution. In the ^{1}H NMR spectrum, the symmetrically equivalent aromatic protons of the zincafluorene framework appeared equivalent as exemplified by the 1- and 8-position protons of the zincafluorene unit, observed at 7.58 ppm (2H, d). This observation indicates the rapid rotation about the C–Zn bond in solution and likely no preference between the two conformations.

Building on the findings for **Z-cAAC^{Cy}**, we next examined the molecular structures of **Z-SIP** and **Z-IP** determined by SC-XRD as shown in Fig. 3a. Although both **Z-SIP** and **Z-IP** crystallize with two crystallographically independent molecules, their geometries are similar (Fig. S3 and S4); therefore, one representative molecule is shown for each structure here for clarity. The ω values for imidazolidine (or imidazole) and zincafluorene rings were smaller (7.4° for **Z-SIP** and 6.7° for **Z-IP**) than that for **Z-cAAC$^{Cy}_{\parallel}$**, indicating an almost coplanar configuration. Consequently, the 1,8-protons in the zincafluorene moiety (H_a, green balls in Fig. 3b) were positioned above the phenyl ring of the 2,6-diisopropylphenyl (Dipp) unit. In the ^{1}H NMR spectrum, **Z-SIP** and **Z-IP** exhibited doublet resonances at $\delta = 6.21$ and 6.27 ppm (2H each), assignable to the H_a, which are substantially upfield from the 7.58 ppm signal of **Z-cAAC^{Cy}**. This pronounced upfield shift is attributed to the ring-current effect of Dipp,[38] indicating that the coplanar geometry observed in the solid state represents the global-minimum configuration in solution, although some rotation about the C–Zn bond may still occur. Theoretical calculations support this interpretation: the Gibbs free-energy difference between the coplanar and perpendicular conformers, defined as $\Delta G = G_{\text{coplanar}} - G_{\text{perpendicular}}$, is very small for **Z-cAAC^{Cy}** (-0.1 kJ mol^{-1}), whereas the corresponding values for **Z-SIP** and **Z-IP** are much larger (-8.4 kJ mol^{-1} and -12.5 kJ mol^{-1}, respectively), showing a clear energetic preference for coplanarity in the NHC systems.

To further clarify the origin of the energetic preference for coplanarity, we performed additional theoretical calculations explicitly examining the role of dispersion effects. In the preceding paragraph, the Gibbs free energies were calculated

including dispersion corrections. In contrast, when the same calculations are carried out without dispersion corrections, the ΔG values shift toward positive values for all complexes (Table S7), leading to a preference for perpendicular configurations. Structural overlays of the coplanar geometries obtained with and without dispersion corrections further reveal that, upon inclusion of dispersion effects, the distance between the Dipp aryl ring and H_a in the zincafluorene unit decreases noticeably (Fig. S12). The corresponding distances with/without dispersion corrections are 2.71 Å/2.86 Å for **Z-cAAC^{Cy}**, 2.64 Å/2.71 Å for **Z-SIP**, and 2.56 Å/2.68 Å for **Z-IP**. Moreover, the difference in ΔG values between calculations with and without dispersion corrections is approximately twice as large for the NHC complexes (**Z-SIP** and **Z-IP**) compared to the cAAC complex (**Z-cAAC^{Cy}**). This trend correlates well with the number of Dipp units, suggesting that the magnitude of the stabilization scales with the number of Dipp–H_a contacts. Taken together, these observations indicate that dispersion effects, most plausibly CH–π interactions between the Dipp aryl ring of the carbene ligand and the H_a in the zincafluorene framework, could play a pivotal role in stabilizing the coplanar geometry. In this sense, the zincafluorene would serve as a key structural unit that effectively enforces coplanarity in these complexes.

Fig. 4a shows the UV-vis absorption spectra of the complexes in toluene solution. **Z-cAAC^{Cy}** displays a broad absorption tail extending to around 500 nm, which is similar to the diffuse reflectance spectrum of the **Z-cAAC$^{Cy}_{\parallel}$** crystal, while **Z-SIP** and **Z-IP** exhibit absorptions at shorter wavelengths. TD-DFT calculations reproduce this trend: the lowest-energy $S_0 \rightarrow S_1$ transitions are calculated at 430 nm for **Z-SIP** and 423 nm for **Z-IP**, in good agreement with the experimental spectra. The second-lowest singlet state (S_2) also contributes to the absorption at the visible-light edge (395 nm for **Z-SIP** and 389 nm for **Z-IP**) and both $S_0 \rightarrow S_1$ and $S_0 \rightarrow S_2$ transitions predominantly involve electronic excitation to the LUMO in all complexes (Tables S8–S11). Visualization of the LUMO distribution indicated that, similar to **Z-cAAC$^{Cy}_{\parallel}$**, both **Z-SIP** and **Z-IP** form an empty C–Zn π orbital (Fig. 4b), which plays a pivotal role in the visible-light absorption. As noted above, the composition analysis shows that the LUMO of **Z-cAAC$^{Cy}_{\parallel}$** comprises 53.4% carbene C(2p) and 8.5% Zn(4p). By contrast, in **Z-SIP** and **Z-IP**, the carbene C(2p) and Zn(4p) orbitals dominate, with the Zn(4p) contribution markedly increased to 12.0% (**Z-SIP**) and 17.1% (**Z-IP**), while the corresponding carbene C(2p) contributions decreased to 37.0% and 28.4%, respectively (Fig. 4b). These results indicate that the higher-lying empty orbitals (see ref. 39) of NHCs (specifically SIPr and IPr in this study) are beneficial for increasing the Zn 4p character in the C–Zn π-type LUMO relative to cAACs, such as cAAC^{Cy}, although such NHCs shift the absorption toward shorter wavelengths (Fig. 4c). In short, forming an empty C–Zn π orbital that effectively engages the Zn center for distinctive visible-light absorption requires an appropriate orientation and energy level-matching between the empty carbene C(2p) and Zn(4p) orbitals.

To examine the influence of the Zn orbital participation on the excited-state dynamics, we performed a series of photoluminescence (PL) measurements for these complexes in toluene. Among them, **Z-IP** exhibited yellow emission with a peak maximum (λ_{PL}) at 555 nm at room temperature (Fig. 4d), although the PL quantum yield (Φ_{PL}) was low (<1%). In contrast, no detectable emission was observed from **Z-cAAC^{Cy}** or **Z-SIP**, which is likely due to accelerated non-radiative decay pathways. In contrast to the solution state, **Z-IP** exhibited bright green PL in the solid crystalline state at room temperature (Fig. 4d), with a λ_{PL} of 511 nm, which was blue-shifted compared with that in solution. This blue shift is ascribed to restricted conformational freedom in the crystal, which reduces excited-state reorganization and shifts the emission to a higher energy. Φ_{PL} was 21%

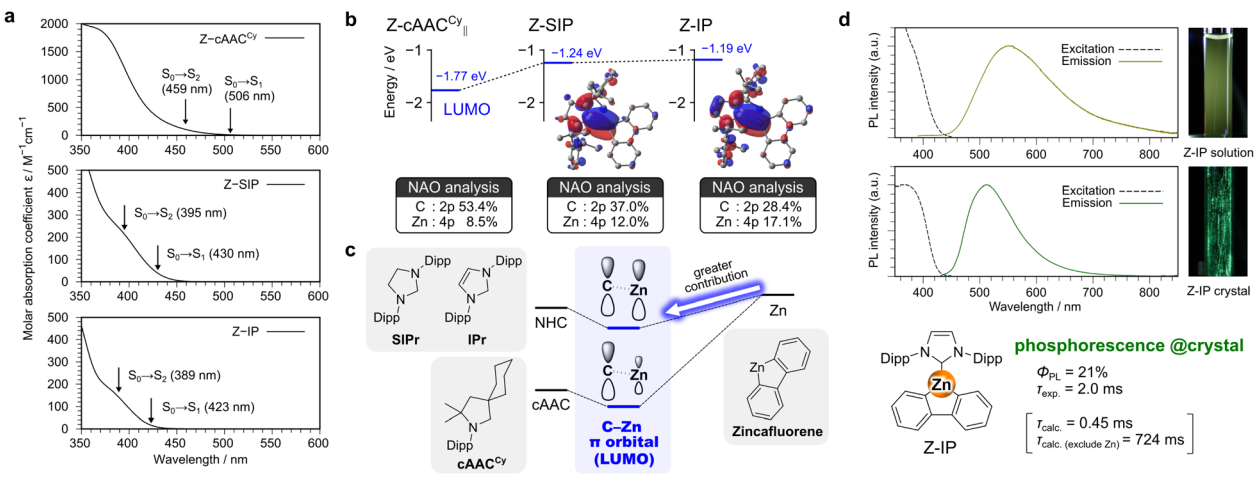

Fig. 4 (a) Experimental UV-vis absorption spectra in 1.0×10^{-3} M toluene solution and theoretically estimated positions of $S_0 \rightarrow S_1$ and $S_0 \rightarrow S_2$ transition indicated by arrows for **Z-cAAC^{Cy}** (top), **Z-SIP** (middle), and **Z-IP** (bottom). (b) LUMO energy levels and NAO compositions for **Z-cAAC^{Cy}**, **Z-SIP**, and **Z-IP**; LUMO isosurfaces for **Z-SIP** and **Z-IP** are shown at an isovalue of 0.03. (c) Schematic of the empty C–Zn π orbital formed between the carbene and zincafluorene units, showing increased Zn(4p) contribution to the LUMO with NHCs. (d) Excitation and emission spectra of **Z-IP** in toluene solution (top) and in the solid crystalline state (bottom) at room temperature. Photographs under black-light illumination are shown on the right. Selected PL parameters for crystalline **Z-IP**, together with computationally estimated emission lifetimes, are listed below.

and PL lifetime ($\tau_{exp.}$) was 2.0 ms. The PL lifetime was too long to be conventional fluorescence, indicating the involvement of the triplet state in the emission process. Additionally, the large energy gap between the excitation and emission spectra supported the attribution of the emissions to phosphorescence. Given that **Z-IP** only consisted of light atoms (H, C, and N) except for the Zn atom, it was reasonable that the heavy atom effect of the Zn center operated through the involvement of the Zn orbital in the excited states.

To gain further insight into the emission mechanism, we performed TD-DFT calculations, including spin–orbit coupling (SOC) (see the SI). When the phosphorescence rate constant (k_{phos}) was evaluated at the lowest triplet (T_1)-optimized geometry, the result largely deviated from the experiment (Table S14). By contrast, the calculation at the S_0-opt geometry gave a k_{phos} of approximately 470 s^{-1}, which corresponds to an estimated observed lifetime ($\tau_{calc.}$) of 0.45 ms when the experimental Φ_{PL} of 21% is taken into account, showing better agreement. We regard the S_0-based estimate as more representative of the crystalline emission, because rigidification in the solid crystalline state suppresses excited-state structural relaxation. When the SOC contribution from the Zn atom was excluded, k_{phos} decreased by more than three orders of magnitude to roughly 0.3 s^{-1}, resulting in a lifetime ($\tau_{calc.(exclude\ Zn)}$) of about 0.7 s. These results highlight the essential role of the Zn center in promoting SOC and governing the room-temperature phosphorescence in **Z-IP**.

Finally, to probe a potential application of the long-lived bright triplet state, we carried out a representative triplet energy-transfer-type photocatalytic isomerization that is commonly used to benchmark the photocatalytic activity of the complex. As summarized in Table 1, irradiation with a 450 nm blue LED in the presence of 5 mol% of **Z-IP** as the photocatalyst converted *trans*-stilbene and its derivatives into their corresponding *cis* isomers. In contrast, only trace conversion was observed in the absence of the photocatalyst, in the dark, or when using the individual fragments of **Z-IP** (biphenyl, IPr, or synthetic intermediate **1a**[40]). These observations indicate that the photoexcited state of **Z-IP**, generated upon absorption of blue light, is responsible for the photocatalytic activity, and suggest that the stilbene isomerization plausibly proceeds *via* energy transfer from the long-lived T_1 state of **Z-IP**. These results confirm that **Z-IP** operates as an active photocatalyst under visible-light excitation.

Table 1 Photoisomerization of *trans*-stilbene derivatives

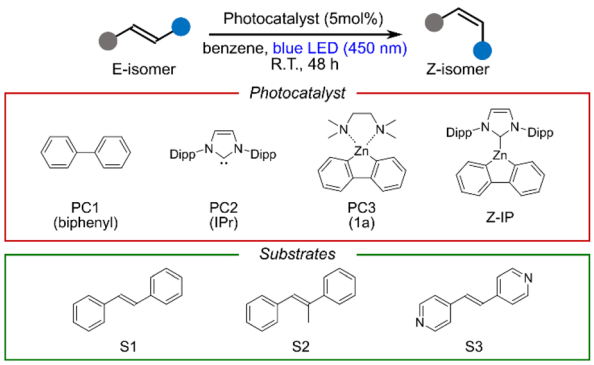

Entry	Photocatalyst	Substrate	LED	Yield (%)
1	—	**S1**	On	Trace
2	**PC1**	**S1**	On	Trace
3	**PC2**	**S1**	On	Trace
4	**PC3**	**S1**	On	Trace
5	**Z-IP**	**S1**	On	64
6	**Z-IP**	**S2**	On	64
7	**Z-IP**	**S3**	On	41
8	**Z-IP**	**S1**	Off	Trace

Conclusions

In conclusion, we developed three mononuclear Zn complexes, **Z-cAAC^{Cy}**, **Z-SIP**, and **Z-IP**, which form empty C–Zn π orbitals engaged in visible-light absorption. Using **Z-cAAC^{Cy}** as a mechanistic probe, selective recrystallization afforded conformational polymorphs, revealing that a coplanar geometry between the carbene and zincafluorene rings enables the formation of an empty C–Zn π orbital as the LUMO, thereby lowering the excitation energy and extending absorption into the visible-light region. Similarly, **Z-SIP** and **Z-IP** form such an empty C–Zn π LUMO under coplanar geometries, achieving visible-light absorption with pronounced Zn-orbital participation in the LUMO. These results demonstrate that appropriate energy-level alignment between the carbene 2p orbital and the Zn 4p orbital, and controlled relative orientation of these orbitals, are the key molecular designs for engaging the Zn center in the low-energy visible-light absorption in mononuclear Zn complexes. Among the three complexes, **Z-IP** displayed bright, long-lived room-temperature phosphorescence, and SOC-inclusive theoretical calculations identify the pivotal role of Zn center in the emission. Moreover, the long-lived excited state of **Z-IP** enabled photoisomerization under blue-light irradiation, further underscoring the non-innocent role of the Zn center in visible-light photofunctions. We believe this study provides clear, mechanistically grounded insight into molecular design strategies for engaging Zn-centered orbitals in visible-light-responsive mononuclear Zn complexes and is expected to accelerate the development of photoactive Zn complexes.

Author contributions

Hidemitsu Iwamoto: investigation (lead); validation (lead); formal analysis (lead); writing – review and editing (lead); writing – original draft (supporting). Yusuke Sunada: funding acquisition (lead); writing – review and editing (equal); methodology (supporting); supervision (supporting); project administration (supporting). Yoshimasa Wada: conceptualization (lead); methodology (lead); formal analysis (equal); investigation (equal); data curation (lead); writing – original draft (lead); visualization (lead); supervision (lead); project administration (lead); funding acquisition (equal).

Conflicts of interest

There are no conflicts to declare.

Data availability

CCDC 2492344 (for **Z-cAAC$^{Cy}_{\perp}$**), 2492350 (for **Z-cAAC$^{Cy}_{\parallel}$**), 2382270 (for **Z-IP**) and 2382271 (for **Z-SIP**) contain the supplementary crystallographic data for this paper.[41a–d]

The supporting data has been provided as part of the supplementary information (SI). Supplementary information: experimental procedures, details of theoretical calculations, Fig. S1–S15, and Tables S1–S14. See DOI: https://doi.org/10.1039/d5sc09340f.

Acknowledgements

This work was supported by JSPS KAKENHI Grant Numbers 23K13757, 24K01495, and 25K01781 (Japan); JST-ALCA-Next Program Grant JPMJAN23B1 (Japan); Fujimori Science and Technology Foundation; and Research Associate Research Fund, Institute of Industrial Science, The University of Tokyo. Computation time was provided by the supercomputer facility of ACCMS at Kyoto University. We are grateful to Dr S. Takizawa (The University of Tokyo) for his assistance with the photophysical measurements.

Notes and references

1 H. Xu, R. Chen, Q. Sun, W. Lai, Q. Su, W. Huang and X. Liu, Recent progress in metal–organic complexes for optoelectronic applications, *Chem. Soc. Rev.*, 2014, **43**, 3259–3302.

2 F. Glaser and O. S. Wenger, Recent progress in the development of transition-metal based photoredox catalysts, *Coord. Chem. Rev.*, 2020, **405**, 213129.

3 C. Forster and K. Heinze, Photophysics and photochemistry with Earth-abundant metals – fundamentals and concepts, *Chem. Soc. Rev.*, 2020, **49**, 1057–1070.

4 R. Jazzar, M. Soleilhavoup and G. Bertrand, Cyclic (Alkyl)- and (Aryl)-(amino)carbene Coinage Metal Complexes and Their Applications, *Chem. Rev.*, 2020, **120**, 4141–4168.

5 O. S. Wenger, Photoactive Complexes with Earth-Abundant Metals, *J. Am. Chem. Soc.*, 2018, **140**, 13522–13533.

6 C. Wegeberg and O. S. Wenger, Luminescent First-Row Transition Metal Complexes, *JACS Au*, 2021, **1**, 1860–1876.

7 V. A. Krylova, P. I. Djurovich, B. L. Conley, R. Haiges, M. T. Whited, T. J. Williams and M. E. Thompson, Control of emission colour with N-heterocyclic carbene (NHC) ligands in phosphorescent three-coordinate Cu(I) complexes, *Chem. Commun.*, 2014, **50**, 7176–7179.

8 M. J. Leitl, V. A. Krylova, P. I. Djurovich, M. E. Thompson and H. Yersin, Phosphorescence versus thermally activated delayed fluorescence. Controlling singlet-triplet splitting in brightly emitting and sublimable Cu(I) compounds, *J. Am. Chem. Soc.*, 2014, **136**, 16032–16038.

9 S. Shi, M. C. Jung, C. Coburn, A. Tadle, M. R. D. Sylvinson, P. I. Djurovich, S. R. Forrest and M. E. Thompson, Highly Efficient Photo- and Electroluminescence from Two-Coordinate Cu(I) Complexes Featuring Nonconventional N-Heterocyclic Carbenes, *J. Am. Chem. Soc.*, 2019, **141**, 3576–3588.

10 R. Hamze, J. L. Peltier, D. Sylvinson, M. Jung, J. Cardenas, R. Haiges, M. Soleilhavoup, R. Jazzar, P. I. Djurovich, G. Bertrand and M. E. Thompson, Eliminating nonradiative decay in Cu(I) emitters: >99% quantum efficiency and microsecond lifetime, *Science*, 2019, **363**, 601–606.

11 N. Ludtke, J. Foller and C. M. Marian, Understanding the luminescence properties of Cu(I) complexes: a quantum chemical perusal, *Phys. Chem. Chem. Phys.*, 2020, **22**, 23530–23544.

12 M. Gernert, L. Balles-Wolf, F. Kerner, U. Muller, A. Schmiedel, M. Holzapfel, C. M. Marian, J. Pflaum, C. Lambert and A. Steffen, Cyclic (Amino)(aryl)carbenes Enter the Field of Chromophore Ligands: Expanded pi System Leads to Unusually Deep Red Emitting Cu(I) Compounds, *J. Am. Chem. Soc.*, 2020, **142**, 8897–8909.

13 J. Li, L. Wang, Z. Zhao, X. Li, X. Yu, P. Huo, Q. Jin, Z. Liu, Z. Bian and C. Huang, Two-Coordinate Copper(I)/NHC Complexes: Dual Emission Properties and Ultralong Room-Temperature Phosphorescence, *Angew. Chem., Int. Ed.*, 2020, **59**, 8210–8217.

14 A. S. Romanov, S. T. E. Jones, Q. Gu, P. J. Conaghan, B. H. Drummond, J. Feng, F. Chotard, L. Buizza, M. Foley, M. Linnolahti, D. Credgington and M. Bochmann, Carbene metal amide photoemitters: tailoring conformationally flexible amides for full color range emissions including white-emitting OLED, *Chem. Sci.*, 2020, **11**, 435–446.

15 L. P. Ravaro, K. P. S. Zanoni and A. S. S. de Camargo, Luminescent Copper(I) complexes as promising materials for the next generation of energy-saving OLED devices, *Energy Rep.*, 2020, **6**, 37–45.

16 W. B. Jensen, The Place of Zinc, Cadmium, and Mercury in the Periodic Table, *J. Chem. Educ.*, 2003, **80**, 952.

17 Y. Wada and Y. Sunada, Spotlight on Zinc: Exploring the Visible Light Responsiveness of Zinc Complexes, *ChemPlusChem*, 2024, **89**, e202400306.

18 T. Sano, Y. Nishio, Y. Hamada, H. Takahashi, T. Usuki and K. Shibata, Design of conjugated molecular materials for optoelectronics, *J. Mater. Chem.*, 2000, **10**, 157–161.

19 Q.-D. Liu, R. Wang and S. Wang, Blue phosphorescent Zn(II) and orange phosphorescent Pt(II) complexes of 4,4′-diphenyl-6,6′-dimethyl-2,2′-bipyrimidine, *Dalton Trans.*, 2004, 2073–2079, DOI: 10.1039/B404905E.

20 R. Sakamoto, S. Kusaka, Y. Kitagawa, M. A. Kishida, M. Hayashi, Y. Takara, M. Tsuchiya, J. Kakinuma, T. Takeda, K. Hirata, T. Ogino, K. Kawahara, T. Yagi, S. Ikehira, T. Nakamura, M. Isomura, M. Toyama, S. Ichikawa, M. Okumura and H. Nishihara, Fluorescent azadipyrrinato zinc(II) complex: hybridisation with a dipyrrinato ligand, *Dalton Trans.*, 2012, **41**, 14035–14037.

21 Y. Sakai, Y. Sagara, H. Nomura, N. Nakamura, Y. Suzuki, H. Miyazaki and C. Adachi, Zinc complexes exhibiting highly efficient thermally activated delayed fluorescence and their application to organic light-emitting diodes, *Chem. Commun.*, 2015, **51**, 3181–3184.

22 J. Xiong, K. Li, T. Teng, X. Chang, Y. Wei, C. Wu and C. Yang, Dinuclear Zn(II) Complexes Exhibiting Thermally Activated Delayed Fluorescence and Luminescence Polymorphism, *Chem.–Eur. J.*, 2020, **26**, 6887–6893.

23 A. N. Gusev, M. A. Kiskin, E. V. Braga, M. A. Kryukova, G. V. Baryshnikov, N. N. Karaush-Karmazin, V. A. Minaeva, B. F. Minaev, K. Ivaniuk, P. Stakhira, H. Ågren and W. Linert, Schiff Base Zinc(II) Complexes as Promising Emitters for Blue Organic Light-Emitting Diodes, *ACS Appl. Electron. Mater.*, 2021, **3**, 3436–3444.

24 B. Goswami, T. J. Feuerstein, R. Yadav, S. Lebedkin, P. J. Boden, S. T. Steiger, G. Niedner-Schatteburg, M. Gerhards, M. M. Kappes and P. W. Roesky, Thermally Activated Delayed Fluorescence and Phosphorescence Quenching in Iminophosphonamide Copper and Zinc Complexes, *Chem.–Eur. J.*, 2021, **27**, 15109–15118.

25 J. A. Kubler, B. Pfund and O. S. Wenger, Zinc(II) Complexes with Triplet Charge-Transfer Excited States Enabling Energy-Transfer Catalysis, Photoinduced Electron Transfer, and Upconversion, *JACS Au*, 2022, **2**, 2367–2380.

26 D. A. Shariaty, J. Schaab, E. McClure, T. Nattikalungal, P. I. Djurovich, S. E. Bradforth and M. E. Thompson, Donor/Acceptor Ligands Based on an o-Terphenyl Motif to Achieve Thermally Activated Delayed Fluorescence in Zn(II) Complexes, *Inorg. Chem.*, 2025, **64**, 1228–1240.

27 Y. Wada, T. Maruchi, R. Ishii and Y. Sunada, Visible Light Responsive Dinuclear Zinc Complex Consisting of Proximally Arranged Two d^{10}-Zinc Centers, *Angew. Chem., Int. Ed.*, 2023, **62**, e202310571.

28 Y. Wada, E. Matsuo and Y. Sunada, Effects of Heavier Congeners on the Structural and Photophysical Properties of Visible-Light-Absorbing Dinuclear Complexes of Group-12 Elements, *Eur. J. Inorg. Chem.*, 2025, **28**, e202400666.

29 N. Lüdtke, J. Kuhnt, T. Heil, A. Steffen and C. M. Marian, Revisiting Ligand-to-Ligand Charge Transfer Phosphorescence Emission from Zinc(II) Diimine Bis-Thiolate Complexes: It is Actually Thermally Activated Delayed Fluorescence, *ChemPhotoChem*, 2023, **7**, e202200142.

30 M. Putscher and C. M. Marian, Polarity-Tunable Luminescence and Intersystem Crossing of a Zinc(II) Diimine Dithiolate Complex, *J. Phys. Chem. A*, 2023, **127**, 8073–8082.

31 N. Ludtke, A. Steffen and C. M. Marian, Finding Design Principles of OLED Emitters through Theoretical Investigations of Zn(II) Carbene Complexes, *Inorg. Chem.*, 2022, **61**, 20896–20905.

32 O. Mrozek, M. Gernert, A. Belyaev, M. Mitra, L. Janiak, C. M. Marian and A. Steffen, Ultra-Long Lived Luminescent Triplet Excited States in Cyclic (Alkyl)(amino)carbene Complexes of Zn(II) Halides, *Chem.–Eur. J.*, 2022, **28**, e202201114.

33 O. Mrozek, M. Mitra, B. Hupp, A. Belyaev, N. Ludtke, D. Wagner, C. Wang, O. S. Wenger, C. M. Marian and A. Steffen, An Air- and Moisture-stable Zinc(II) Carbene Dithiolate Dimer Showing Fast Thermally Activated Delayed Fluorescence and Dexter Energy Transfer Catalysis, *Chem.–Eur. J.*, 2023, **29**, e202203980.

34 S. Koop, O. Mrozek, L. Janiak, A. Belyaev, M. Putscher, C. M. Marian and A. Steffen, Synthesis, Structural Characterization, and Phosphorescence Properties of Trigonal Zn(II) Carbene Complexes, *Inorg. Chem.*, 2024, **63**, 891–901.

35 M. Mitra, O. Mrozek, M. Putscher, J. Guhl, B. Hupp, A. Belyaev, C. M. Marian and A. Steffen, Structural Control of Highly Efficient Thermally Activated Delayed Fluorescence in Carbene Zinc(II) Dithiolates, *Angew. Chem., Int. Ed.*, 2024, **63**, e202316300.

36 M. J. Frisch, G. W. Trucks, H. B. Schlegel, G. E. Scuseria, M. A. Robb, J. R. Cheeseman, G. Scalmani, V. Barone, G. A. Petersson, H. Nakatsuji, X. Li, M. Caricato, A. V. Marenich, J. Bloino, B. G. Janesko, R. Gomperts, B. Mennucci, H. P. Hratchian, J. V. Ortiz, A. F. Izmaylov, J. L. Sonnenberg, D. Williams-Young, F. Ding, F. Lipparini, F. Egidi, J. Goings, B. Peng, A. Petrone, T. Henderson, D. Ranasinghe, V. G. Zakrzewski, J. Gao, N. Rega, G. Zheng, W. Liang, M. Hada, M. Ehara, K. Toyota, R. Fukuda, J. Hasegawa, M. Ishida, T. Nakajima, Y. Honda, O. Kitao, H. Nakai, T. Vreven, K. Throssell, J. A. Montgomery Jr, J. E. Peralta, F. Ogliaro, M. J. Bearpark, J. J. Heyd, E. N. Brothers, K. N. Kudin, V. N. Staroverov, T. A. Keith, R. Kobayashi, J. Normand, K. Raghavachari, A. P. Rendell, J. C. Burant, S. S. Iyengar, J. Tomasi, M. Cossi, J. M. Millam, M. Klene, C. Adamo, R. Cammi, J. W. Ochterski, R. L. Martin, K. Morokuma, O. Farkas, J. B. Foresman and D. J. Fox, *Gaussian 16 Rev. C.01*. Gaussian, Inc., Wallingford, CT, 2016.

37 The total Zn(4p) contribution of 2.1% can be decomposed into 0.4% and 1.7% contributions from the in-plane and out-of-plane 4p orbitals relative to the zincafluorene plane, respectively. The in-plane Zn(4p) component, which is associated with the zincafluorene σ(Zn–C) orbital, may partly contribute to an antibonding interaction with the carbene 2p orbital, leading to destabilization of the LUMO energy in **Z-cAAC^{Cy}**$_{\perp}$. However, given its small magnitude, this destabilizing contribution is considered to be relatively minor in contributing to the LUMO energy difference between **Z-cAAC^{Cy}**$_{\perp}$ and **Z-cAAC^{Cy}**$_{\parallel}$.

38 V. A. Krylova, P. I. Djurovich, J. W. Aronson, R. Haiges, M. T. Whited and M. E. Thompson, Structural and Photophysical Studies of Phosphorescent Three-Coordinate Copper(I) Complexes Supported by an N-Heterocyclic Carbene Ligand, *Organometallics*, 2012, **31**, 7983–7993.

39 This general trend, namely that NHCs typically possess higher-lying LUMO levels than cAACs, has been well summarized in a review article (see Fig. 2 and 3 in the following reference): S. Kumar Kushvaha, A. Mishra, H. W. Roesky and K. Chandra Mondal, Recent Advances in the Domain of Cyclic (Alkyl)(Amino) Carbenes, *Chem.–Asian J.*, 2022, **17**, e202101301.

40 M. Gast, J. Anton and G. Linti, Synthesis of 9-Gallafluorenes via Group 12 Metal Biphenylenes, *Eur. J. Inorg. Chem.*, 2018, 4074–4083.

41 (*a*) CCDC 2492344: Experimental Crystal Structure Determination, 2026, DOI: 10.5517/ccdc.csd.cc2pnh62; (*b*) CCDC 2492350: Experimental Crystal Structure Determination, 2026, DOI: 10.5517/ccdc.csd.cc2pnhd8; (*c*) CCDC 2382270: Experimental Crystal Structure Determination, 2026, DOI: 10.5517/ccdc.csd.cc2kyyfx; (*d*) CCDC 2382271: Experimental Crystal Structure Determination, 2026, DOI: 10.5517/ccdc.csd.cc2kyygy.